

NUMERICAL INVESTIGATION OF HEAT TRANSFER PERFORMANCE OF SYNTHETIC JET IMPINGEMENT ONTO DIMPLED/PROTRUSIONED SURFACE

by

Di ZHANG*, **Ke YANG**, **Huan-Cheng QU**, and **Ji GAO**

School of Energy and Power Engineering, Xi'an Jiaotong University, Xi'an, China

Original scientific paper
DOI: 10.2298/TSC15S1S21Z

Dynamic mesh methods and user defined functions are adopted and the shear stress transport $k-\omega$ turbulent model has been used in the numerical investigation of heat transfer performance of synthetic jet impingement onto dimple/protrusioned surface. The results show that the local time-averaged Nusselt number of the dimpled/protrusioned target surface tends to be much closer with that of flat cases with increasing of frequency. The heat transfer performance gets better when frequency increases. The area-averaged time-averaged Nusselt number of protrusioned target surface is the most close to that of flat cases when $f = 320$ Hz while it is the smallest among the synthetic jet cases in dimpled target surface. The heat transfer enhancement performance of synthetic jet is 30 times better than that of natural convection. The time-averaged Nusselt number of stagnation point in the protrusioned target surface is higher than that of flat target surface while it is lower in the dimpled surface than that of flat surface no matter in the synthetic jet, steady jet or natural convection cases. Meanwhile, the time-averaged Nusselt number of stagnation point in the synthetic jet cases increases with the increasing of frequency. It is worth pointing out that the time-averaged Nusselt number of stagnation point is lower than that of steady cases when the frequency is low. However, it shows a bit higher than that of steady cases when $f = 320$ Hz.

Key words: *synthetic jet, dimpled/protrusioned target, heat transfer enhancement*

Introduction

Impinging jets have wide applications such as the cooling of gas turbine blades and drying of papers and textiles, due to its high heat transfer coefficient near the stagnation zone. A great deal of investigation has been conducted including the effect of Reynolds number, jet angle, jet-to-plate spacing, and jet shape on the flow and heat transfer in the jet impingement.

Synthetic jet is one kind of jet and it is widely used in the flow separation control of boundary layer [1] in the last few decades due to that it induces perturbation into mainstream. It is also named as zero-net mass flux jet produced by the momentary ejection and suction of fluid across the orifice and so the net mass flux is zero. The cooling performance of confined impinging synthetic jet ($Re_j = 2210$ and 3300 , $H/d = 2, 4$, and 8 , $f = 30, 80, 160$, and 250 Hz) was investigated experimentally by Vukasinovic *et al.* [2] in 2003. The countercurrent radial flow is induced in the gap and strong vorticity diffusion gets into thermal boundary layer resulting to

* Corresponding author; e-mail: zhang_di@mail.xjtu.edu.cn

the mixing enhancement. Arik *et al.* [3, 4] conducted the experimental investigation on the heat transfer performance of synthetic jet and pointed out that the optimal heat transfer coefficient was obtained with the resonance frequency. The cooling performance of synthetic jet shows 30% and 40% better than that of steady jet with optimal and the same jet-to-target spacing, respectively. Valiorgue *et al.* [5] performed the experimental investigation on the cooling performance of round impinging synthetic jet by PIV and thermal imaging camera ($1000 < Re_j < 4300$, $H/d = 2$, $1 < L_0/D < 22$). Chaudhari *et al.* [6, 7] carried out the experimental study about the heat transfer performance of both single and multiple impinging synthetic jets ($950 < Re_j < 4200$, $0 < H/d < 25$, $100 < f < 400$ Hz) in the application of heat sink with fans and crossflow. The results indicate that the heat transfer performance of synthetic jet would be higher than that of continuous flow with higher Reynolds number. Tan *et al.* [8] experimentally studied the heat transfer characteristics of synthetic jet driven by piezoelectric actuator.

Dimple and protrusion are one kind of concavities which have significant enhancement in heat transfer with low penalty in pressure drop. Lots of scholars have conducted the heat transfer enhancement of jet impinging onto dimpled/protrusioned surface. Eight-by-eight jet arrays impinging onto a staggered array of dimples ($Re_j = 11,500$, $H/d = 2, 4$, and 8) was investigated by Kanokjaruvijit *et al.* [9]. The maximum crossflow scheme and larger H/d impingement onto dimpled surface performs much better compared to the plate. Wall-resolved and zonal numerical large eddy type simulation are performed for impingement onto a dimpled surface at $Re_j = 23,000$ [10]. The cooling characteristics of dimpled and smooth heated surfaces subjected to co-axial impinging jet were compared with $Re_j = 10,000, 20,000$, and $40,000$, and H/d from 1 to 10 [11] and results shows that the average Nusselt number increases with dimpled surface by up to 6% over the whole surface area comparing to the smooth surface.

According to this literature review, both of the methods involved including synthetic jet and dimple/protrusion can augment the heat transfer of impinging jet significantly. The heat transfer performance is deduced to be improved further if the synthetic jet and dimple/protrusion are used together. However, there is no such kind study about this subject. So the present work mainly explores the flow and heat transfer performance of synthetic jet impinging onto dimpled/protrusioned surface.

Numerical model

As shown in fig. 1, the piston-based synthetic jet actuator was used for the generation of the velocity pulsation. The flat target surface was arranged in some distance with the orifice of jet. The dimple and protrusion were located with the centerline parallel with the center of synthetic jet.

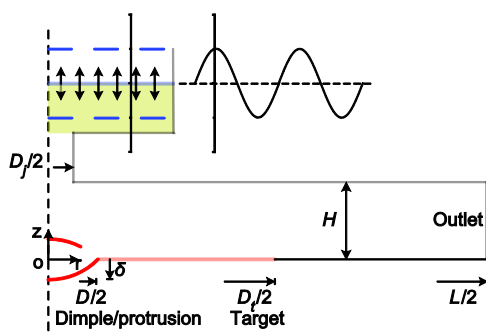


Figure 1. Sketch of computational domain and boundary condition

The whole geometry model is axisymmetric as same as in [2]. The colored region is presented as the cavity of synthetic jet. The moving type of the diaphragm in the piston was assumed to be sinusoidal. The diameter of orifice is D_j , the jet-to-target spacing is $H/D_j = 4$. The diameter of dimple and protrusion is the same as $D/D_j = 2$, and the depth is $\delta/D = 0.2$. The diameter of heated target surface is $D_t/D_j = 13.6$, and the diameter of whole target surface is $L/D_j = 25$. Air was used as the working fluid with $Pr = 0.71$ due to its low cost, availability and reliability.

Non-slip wall boundary condition with constant heat flux q was applied on the target surface which was marked in red color as shown in fig. 1. Dimpled/protrusioned surface was also with the same condition when the dimple/protrusion was arranged on the target surface. Adiabatic no-slip wall boundary was used for the confined wall while the pressure boundary was applied at the outlet surface.

In the computation, the law of diaphragm motion is defined, namely the magnitude and frequency of motion. The motion displacement S is defined as:

$$S = A \sin(2\pi ft) \quad (1)$$

The circular movement of diaphragm leaves the region of cavity increases and decreases constantly. The dynamic mesh was adopted for the movement and the variation of motion was defined by user defined function embedded in the program. The structural grid was performed for the whole computational region. The layering method was used for the grid generation, which does not affect the initial distribution of grid and provides good quality of grid in the motion.

The velocity of the jet is low and so the fluid is treated as incompressible flow. RANS methods were adopted to deal with the flow and heat transfer equations. QUICK scheme was used for the convective term. Central difference form was used for diffusion term. The PISO algorithm was applied for the coupling between pressure and velocity. Shear stress transport (SST) $k-\omega$ turbulent model was more acceptable in the unsteady computation of synthetic jet. In the present numerical work, the realizable $k-\varepsilon$ turbulent model coupled with enhanced wall function, SST turbulent model coupled with $\gamma-\theta$ transition model, and SST $k-\omega$ turbulent model were compared with the experimental result [2] as shown in fig. 2. The difference between experimental result and realizable $k-\varepsilon$ as well as SST + $\gamma-\theta$ turbulent model is large. By contrast, the local heat transfer coefficient of SST $k-\omega$ turbulent model is much closer to the experimental result. Among them, SST $k-\omega$ turbulent model was the most suitable method to simulate the synthetic jet impingement.

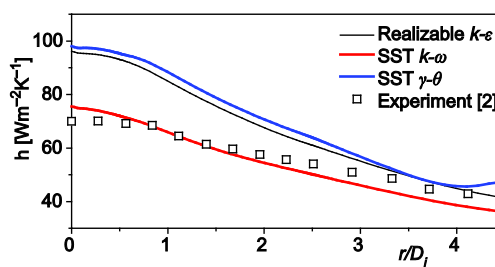


Figure 2. The experimental validation of turbulent model (for color image see journal web-site)

Result and discussion

Figure 3 demonstrates the velocity contour and streamlines for flat target surface, protrusioned surface and dimpled surface for the case of $f = 80$ Hz, and four moments of $t = 0.25 \tau$, 0.5τ , 0.75τ , and τ are considered. As observed in the figure, the flow shows the same pattern at different moments. When the vibrating diaphragm moves to the right end at $t = 0.25 \tau$, the flow velocity at the jet is zero, and it is in the process of changing from positive value to negative one. Being influenced by the former cycle, the flow around the centerline continues impinging to the target surface, while the flow around the jet begins to enter the cavity. In the case of flat target surface, the flow turns to be wall jet after the rotation of 90° , and then it moves on in the radial direction. For the dimpled surface the flow moves along the surface, and then it develops in the radial direction. In the case of protrusioned surface, the flow moves along the surface in the impingement and then it moves to the downstream. At $t = 0.5 \tau$

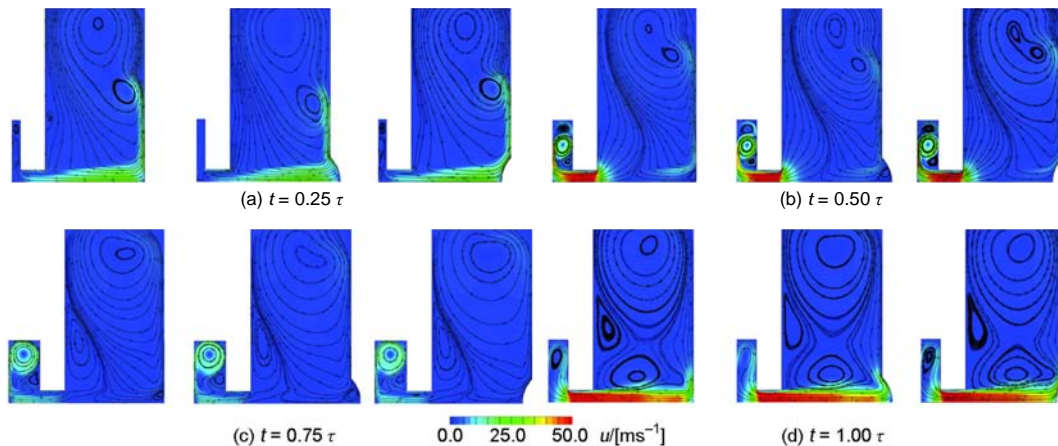


Figure 3. Velocity contours and streamline for $f = 80$ Hz (left: flat, center: dimpled, right: protruded)
(for color image see journal web-site)

the vibrating diaphragm moves to the mean piston, and the flow velocity at the jet reaches the minimum negative value. The flow is inhaled into the cavity mainly from the confined surface, and different sizes of vortices can be observed on the target surface. For the flat surface, a small vortex occurs at the stagnation point, and a notable vortex can be observed in the dimple for the dimpled surface. While for the case of protruded surface no vortex occurs around the protrusion. The vibrating diaphragm moves to the left end at $t = 0.5 \tau$, and the suction process ends. Except for the velocity fluctuation of flow in the cavity, the flow velocity in the confined space is almost zero. Besides, at this moment a large-scale vortex is observed at the confined surface. Then the blow process begins, and at $t = 1.00 \tau$ the vibrating diaphragm moves to the mean position, where the flow velocity at the jet reaches the maximum value. The increasing flow velocity induces a notable increase in the angle between the flow direction and the flat surface. A small size of vortex occurs around the dimple edge, and this has negative effect on the heat transfer performance. According to the discussions, it can be found that the best impingement effect occurs in the blow process ($t = 0.75 \tau - 1.25 \tau$), during which the flow velocity at the spout is positive, and the flow directly impinges on the center of the target surface.

Figure 4 shows the variation of averaged Nusselt number (Nu) with time in two cycles for flat target surface. As observed in the figure, Nu varies periodically for the three types of synthetic jet frequency. In the blow process, Nu increases, meaning that it increases with the flow velocity at the jet. In the suction process, Nu is relatively low, and the minimum mean occurs when the jet velocity reaches the highest value. As the jet frequency increases from $f = 80$ Hz to $f = 160$ Hz, a notable increase in Nu can be observed, and the increase is more obvious in the blow process. As the jet frequency increases from $f = 160$ Hz to $f = 320$ Hz, a further increase of Nu occurs. Note that at the beginning of the blow process, a slight variation of Nu occurs, and a small peak value occurs at $f = 320$ Hz. This is because that the increasing jet frequency leads to an increase in the flow pulsation at the jet. Under this condition, the flow temperature around the jet is relatively low. With the rapid increase in flow velocity at the jet, the flow with low temperature around the jet develops to a larger scale in the axis direction, and this induces the small fluctuation of Nu at high jet frequency.

Figure 5 shows the variation of mean Nusselt number with time for flat target surface, protruded surface, and dimpled surface at $f = 80$ Hz. It is found that the application of

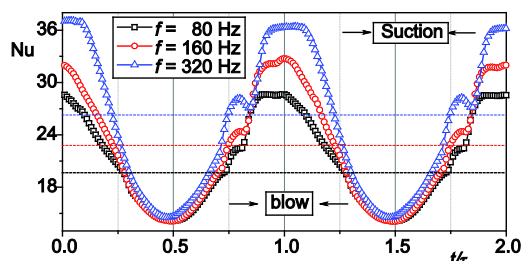


Figure 4. Averaged Nusselt number variation in flat cases (for color image see journal web-site)

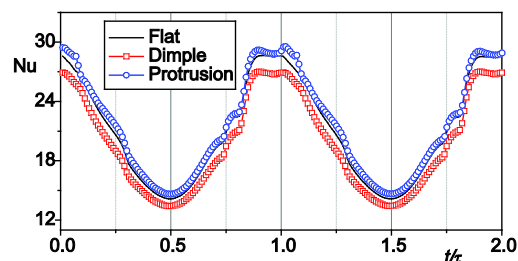


Figure 5. Averaged Nusselt number variation for $f = 80$ Hz (for color image see journal web-site)

protrusion and dimple has notable effect on the cooling effect. Compared with the case of flat target surface, the use of dimple induces a systematical decrease of Nu. From fig. 3 it can be found that the dimpled surface leads to a larger scale of vortex in the suction process, thus having negative effect on the heat transfer performance. While in the blow process the application of dimple increase the distance between the jet and the target surface, and this also has negative effect on the heat transfer process. Nu of protrusioned surface is slightly higher than that of smooth surface, especially during the blow process. According to the fig. 3, at $t = 1.00 \tau$ the flow velocity reaches its maximum value, and the jet is closer to the protrusioned surface. The boundary layer on the protrusioned surface is very thin when the jet develops in the radial direction, and this is beneficial to the heat transfer performance. As a result, Nu of protrusioned surface is higher than that of flat surface.

The averaged Nusselt number Nu variation of target surface with time for $f = 160$ Hz is shown in fig. 6. The Nu variation in three cases shows the same tendency and Nu varies in sinusoidal type with jet velocity. Moreover, Nu shows higher value in blow process than that in suction process. Nu in dimple case is lower than that in flat case, which is in accordance with that for $f = 80$ Hz. The main reason is that the size of the vortex inside the dimple is enlarged by dimple in the jet suction process and so the heat transfer is worsened. While the distance between the jet and target surface is further when the dimple is arranged in the jet blow process resulting in heat transfer deterioration. The Nu variation shows the different tendency in protrusion case. Nu of protrusioned target surface is similar with flat case in jet suction process. However, in jet blow process, Nu of protrusioned target surface is lower than that in flat case, especially when the jet velocity comes to the maximum. In the development of jet velocity on the centerline, two peak values of jet velocity are formed in the flat target surface and dimpled target surface. Because the distance is shortened by the protrusion, the second peak value of jet velocity disappeared, which results in lower heat transfer performance than flat case. Although, the heat transfer performance of protrusioned target surface is still better than dimpled target surface.

Figure 7 shows the variation of averaged Nusselt number of target surface with time in flat case and dimple/protrusion case at $f = 320$ Hz. The variation of Nu shows the same tendency for different target surfaces. The Nu shows the higher value in jet blow process while it shows lower value in jet suction value, varies in sinusoidal type as jet velocity variation. At the beginning of the jet blow process, Nu shows slightly fluctuated. The main reason is that fluid with relatively low temperature is entrained near the jet and it develops in the axial direction when the jet velocity increases sharply, which makes that the Nusselt number shows the fluctuating magnitude. Nu in dimple case is lower than that in flat case and the reason is as discussed before. Meanwhile, Nu of protrusioned target surface is the same value as

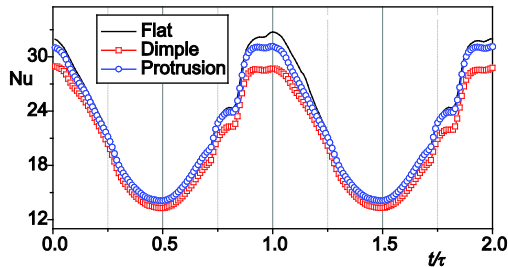


Figure 6. Averaged Nusselt number variation for $f = 160$ Hz (for color image see journal web-site)

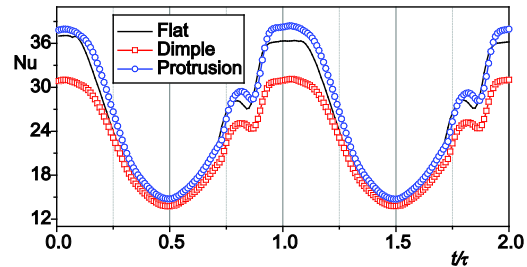


Figure 7. Averaged Nusselt number variation for $f = 320$ Hz (for color image see journal web-site)

that in flat case for jet suction process and shows higher value than that in flat case for jet blow process. The reason is that the frequency is much higher than the other frequency, so the pulsating distance gets shortened in the same Reynolds number. The jet velocity just shows the only one peak value in the axial direction. The distance between jet and target surface is reduced by protrusion and the dissipation of energy is also reduced, so the heat transfer performance gets better.

The local time-averaged Nusselt number (Nu_c) distribution of target surface in natural convection and steady jet as well as synthetic jet was shown in fig. 8. It is clearly seen that Nu_c in steady jet and synthetic jet is more than times higher than that in natural convection. In the natural convection, Nu_c in the flat cases decreases monotonously from the stagnation point in the radial direction. After arrangement of protrusion, Nu_c near the protrusion region shows big value compared with flat target. It decreases from the stagnation point and comes to the similar value with flat case near the edge region. However, the main change occurs near the dimple region after arrangement of dimple. Nu_c near the stagnation region of dimple case shows lower value compared with that in flat case while it increases along with the radial direction and comes to the same value with flat case at the edge of dimple. Nu_c at the stagnation point in protrusion case is the biggest among different cases and it is the lowest in the dimple case. In the steady jet, Nu_c in the flat case increases firstly in the radial direction and forms the maximum when $r/D_j = 0.5-1.0$. Then Nu_c decreases in the radial direction. After arrangement of dimple, Nu_c at the stagnation point is lower than that in flat case. Then it increases along with the radial direction and shows the maximum when reaching the dimple edge. Because of the small flow separation outside of dimple edge, Nu_c forms the local minimum firstly and re-

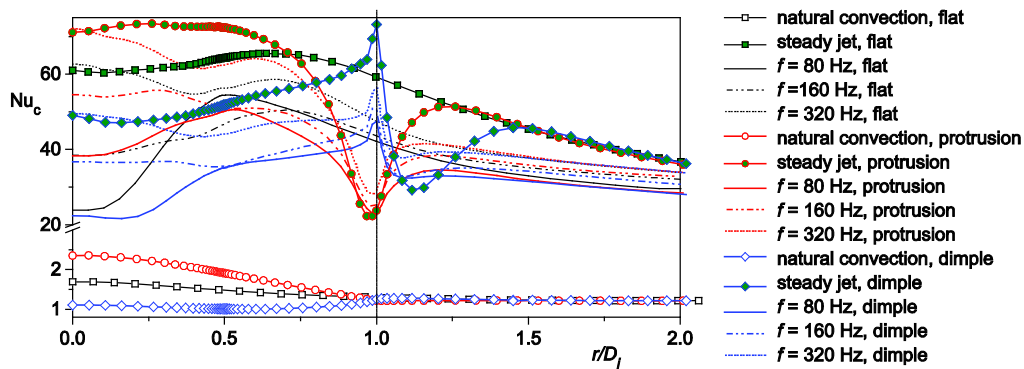


Figure 8. Local time-averaged Nusselt number distribution (for color image see journal web-site)

turns to the value as flat case along with the radial direction. The distance between jet and target is shortened when the protrusion was arranged and Nu_c in the stagnation point is higher than that of flat case. The flow separation occurs near the protrusion edge, so the heat transfer is worsened and Nu_c shows the lowest value and it returns to the value as flat case along with the radial direction. Nu_c variations for synthetic jet are similar with the above description and the mainly difference exists for the stagnation region with $f = 320$ Hz, namely that Nu_c of stagnation point shows the peak value. The reason is that the jet flow is much easily affected by the movement of cavity and its temperature is the averaged value of blow and suction process. In Nu_c definition, the reference temperature, T_c , the local fluid temperature is relatively higher, which higher Nu_c is derived. Moreover, no matter in flat cases or dimple/protrusion cases, Nu_c is more close to the distribution of steady jet when the frequency increases. The heat transfer is enhanced with the increasing of frequency for synthetic jet cooling.

The area-averaged time-averaged Nusselt number Nu_{av} was shown in fig. 9. The frequency was plotted in the horizontal axis. Nu_{av} keeps constant in the steady jet and natural convection. The heat transfer of target surface was enhanced by the protrusion and it was worsened by the dimple in the natural convection. However, the heat transfer is enhanced near the stagnation region and worsened near the edge of protrusion in the steady jet cases. Nu_{av} of protrusioned target surface is slightly lower than that of flat target surface in the area-averaged calculation of axisymmetrical model. Meanwhile, the heat transfer is worsened in both the stagnation region and the region outside the edge for the dimpled target surface. The overall Nu_{av} of dimpled surface is 8.5% lower than that for flat cases. The heat transfer performance of synthetic jet is improved 30 times compared with natural convection. Nu_{av} of synthetic jet increases monotonously with the increasing of frequency and the difference with steady jet is decreases in the same tendency. Nu_{av} of protrusioned target surface is slightly lower than that of flat cases and as the frequency increases, the difference between them decreases. The smallest difference is 0.8% when $f = 320$ Hz. Nu_{av} of dimpled target surface is lowest in the synthetic jet. The difference of Nu_{av} between dimpled and flat target surface decreases as frequency increases. It changes from 11.3% for $f = 80$ Hz to 2.3% for $f = 320$ Hz.

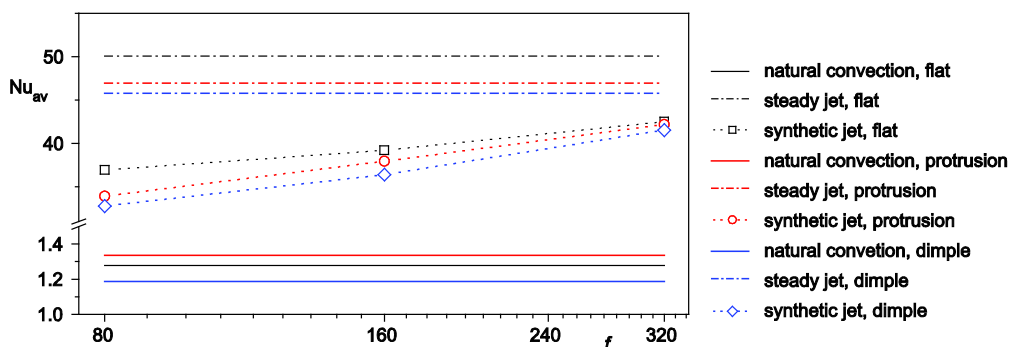


Figure 9. Area-averaged time-averaged Nusselt number (for color image see journal web-site)

The variations of time-averaged Nusselt number of stagnation point $Nu_{c,s}$ with frequency are shown in fig. 10. $Nu_{c,s}$ in protrusioned cases shows the greatest value in the comparison no matter in natural convection, steady jet or in synthetic jet. Besides, $Nu_{c,s}$ in dimpled cases shows the smallest value. The $Nu_{c,s}$ in synthetic jet cases increases with the increasing of frequency. It is worthy pointing out that the $Nu_{c,s}$ in lower frequency shows lower value compared with that in steady cases while it is slightly higher with $f = 320$ Hz than that in steady cases.

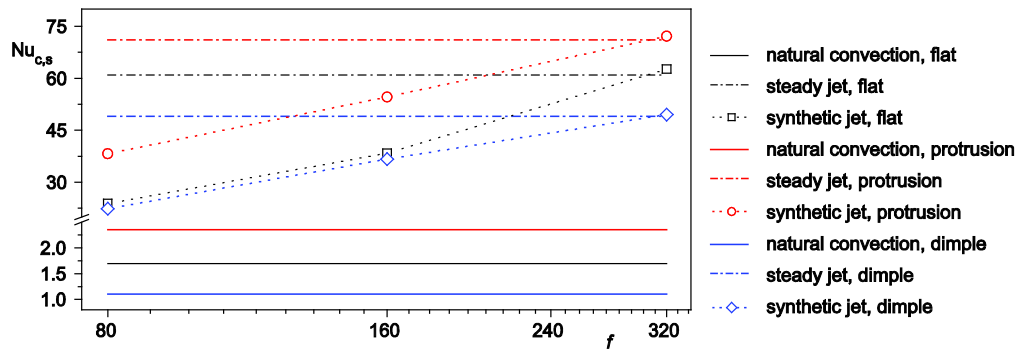


Figure 10. Time-averaged Nusselt number of stagnation point (for color image see journal web-site)

Conclusions

The dynamic mesh has been adopted in the numerical investigation of heat transfer performance of synthetic jet impinging onto dimpled/protrusioned target surface. The effect of pulsating frequency on the cooling performance was studied and the result of synthetic jet has been compared with that of natural convection and steady jet. The following conclusions were drawn.

- The local time-averaged Nusselt number of target surface in different shapes is more similar to that of steady jet with the increasing of frequency for the synthetic jet impingement, which indicates that the heat transfer performance of synthetic jet is enhanced as the frequency increases. The area-averaged time-averaged Nusselt number of target surface in synthetic jet impingement increases with the increasing of frequency. Meanwhile, Nu_{av} difference between synthetic jet and steady jet is reduced when the frequency increases. The difference is only 0.8% when $f = 320$ Hz for protrusion and flat case. Nu_{av} of dimple case is the lowest in which the difference with flat case is 2.3% when $f = 320$ Hz. Compared with natural convection, the heat transfer is enhanced by near 30 times for synthetic jet impingement.
- No matter in natural convection, steady jet or in synthetic jet, the time-averaged Nusselt number of stagnation point of protrusion case is higher than that in flat case while it shows lower value in dimple case. The time-averaged Nusselt number of stagnation point increases with the increasing of frequency. It is worthy pointing out that when the frequency is low, the time-averaged Nusselt number in the synthetic jet is lower than that in steady jet. However, the frequency is as high as $f = 320$ Hz, the time-averaged Nusselt number in synthetic jet shows higher value than that in steady jet impingement.

Nomenclature

D – dimple diameter, [m]
 D_j – jet diameter, [m]
 f – frequency, [Hz]
 H – jet-to-target spacing, [m]
 L – length of target surface, [m]
 L_0 – stoke length, [m]
 Nu – Nusselt number
 q – heat flux, [Jm^{-2}]

Re – Reynolds number
 S – motion displacement, [m]
 ΔT – temperature difference, [K]
 U_0 – time-averaged jet exit velocity, [ms^{-1}]

Greek symbols

δ – depth of dimple, [m]
 τ – period of the cycle, [s]

References

- [1] You, D., et al., Active Control of Flow Separation over an Airfoil Using Synthetic Jets, *Journal of Fluids and Structures*, 24 (2008), 8, pp. 1349-1357
- [2] Vukasinovic, J., et al., Spot-Cooling by Confined, Impinging Synthetic Jet, *Proceedings*, HT2003, ASME Summer Heat Transfer Conference, Las Vegas, Nev., USA, HT2003-47245, 2003
- [3] Arik, M., Local Heat Transfer Coefficients of a High-Frequency Synthetic Jet during Impingement Cooling over Flat Surfaces, *Heat Transfer Engineering*, 29 (2008), 9, pp. 763-773
- [4] Arik, M., et al., Steady and Unsteady Air Impingement Heat Transfer for Electronics Cooling Applications, *Journal of Heat Transfer*, 135 (2013), 11, pp. 111009-111009
- [5] Valiorgue, P., et al., Heat Transfer Mechanisms in an Impinging Synthetic Jet for a Small Jet-to-Surface Spacing, *Experimental Thermal and Fluid Science*, 33 (2009), 4, pp. 597-603
- [6] Chaudhari, M., et al., Heat Transfer Characteristics of Synthetic Jet Impingement Cooling, *International Journal of Heat and Mass Transfer*, 53 (2010), 5-6, pp. 1057-1069
- [7] Chaudhari, M., et al., Heat Transfer Characteristics of a Heat Sink in Presence of a Synthetic Jet, *Components, Packaging and Manufacturing Technology, IEEE Transactions*, 2 (2012), 3, pp. 457-463
- [8] Tan, X., et al., Flow and Heat Transfer Characteristics under Synthetic Jets Impingement Driven by Piezoelectric Actuator, *Experimental Thermal and Fluid Science*, 48 (2013), July, pp. 134-146
- [9] Kanokjaruvijit, K., et al., Jet Impingement on a Dimpled Surface with Different Crossflow Schemes, *International Journal of Heat and Mass Transfer*, 48 (2005), 1, pp. 161-170
- [10] Jefferson-Loveday, R. J., et al., LES of Impingement Heat Transfer on a Concave Surface, *Numerical Heat Transfer, Part A: Applications*, 58 (2010), 4, pp. 247-271
- [11] Celik, N., Effects of the Surface Roughness on heat Transfer of Perpendicularly Impinging co-Axial Jet, *Heat and Mass Transfer*, 47 (2011), 10, pp. 1209-1217